Optimizing Pump-and-Treat method by using optimization-simulation models

Mohammad Javad Zeynali[*a] , Mohammad Nazeri Tahroudi[b], Omolbani Mohammadrezapour[c]

[a] Department of Civil Engineering, Faculty of Engineering, University of Torbat-Heydarieh (UTH), Torbat-Heydarieh, Iran
[b] Department of Water Engineering, Faculty of Agriculture, Lorestan University, Khorramabad, Iran
[c] Department of Water Engineering, Faculty of Water and Soil Engineering, Gorgan University of Agricultural Sciences and Natural Resources, Gorgan, Iran

ABSTRACT

The goals of this research include investigating the efficiency of the finite element method and its combination with meta-heuristic algorithms to solve the optimization problem of the pump and treat (PAT) system. In this research, the hybrid optimization-simulation models were developed to determine the optimal groundwater remediation strategy using the pump and treat (PAT) system. The results indicated that when we consider minimizing the contaminant in groundwater at the end of the remediation period as the objective function, locating the pumping wells in the path of the contaminant flow and close to the contaminant source. In a single objective problem, the GA-FEM model with an average value of 0.0005036 in five runs of the model had the best performance among other models. The results of the two-objective problem indicated that MOMVO-FEM, despite a few solutions in optimal Pareto-front, could find a better location for pumping wells. Finally, it can be said that among factors such as the location of pumping wells and pumping rate, the most influential factor in choosing the right pumping and treatment policy is the proper location of pumping wells. Also, the location of contamination pumping wells does not necessarily correspond to the location of the contamination seepage.

ARTICLE INFO

1. Introduction

The main sources of groundwater contamination can be from natural or human-made sources. Natural resources can include sea water intrusion, decomposition of natural minerals in the earth's crust, and landslides (Eldho and Swathi, 2018). In recent decades, groundwater quality has been severely affected due to improper use and management of groundwater resources. The human-made sources are plenty ranging from domestic sources like leakages from septic tanks and sewers, improper disposal of industrial waste, widespread use of chemicals in agriculture such as fertilizers and pesticides and many other human activities (Freeze and Cherry, 1979).

As mentioned, other sources of pollution include improper disposal of waste. When landfills are not well insulated, waste leachate that contains hazardous materials such as heavy metals can easily percolate into groundwater and contaminate it (Eldho and Swathi, 2018). Groundwater contamination and reducing groundwater quality have made groundwater remediation and better management an urgent need. Over the past few decades, groundwater pollution has become a major problem in many parts of the world. In many parts of the world, available groundwater is unsuitable for drinking and even agriculture. Besides, groundwater remediation methods, are very expensive. Therefore, in choosing the remediation method,

an appropriate approach should be taken so that the contamination is effectively removed and the proper result is finally achieved. Therefore, optimization is very important in groundwater remediation (Eldho and Swathi, 2018). In the discussion of groundwater pollution, Darabi and Ghafouri, (2007) and Guneshwor et al. (2018) have identified sources of pollutants and some other researchers have studied various methods of groundwater remediation such as in situ phytoremediation Kumar et al. (2015) and Mategaonkar et al. (2018) or pump and treatment method (Wang et al., 2018). However, the design of an efficient remediation system is done for various purposes. Remediation methods generally have many influential components. For example, the pump and treatment method has important components such as the position of the pumping well, the rate of pumping, the remediation time and the rate of groundwater drawdown during pumping. Different methods are used to solve the optimizing problem of groundwater remediation. Some researchers have used nonlinear programming method (Gorelick et al., 1984) or meta-heuristic algorithms such as AMALGAM (Ouyang et al., 2017), NSGA-II (Akbarpour et al., 2020), probabilistic multi objective genetic algorithm (PMOGA) (Singh et al., 2008), niched Pareto genetic algorithm (Erickson et al., 2002). One of the most important goals of groundwater remediation is to reduce the contaminant concentration to the permissible level. The carcinogenic human health risk can be directly or indirectly related to the contaminant concentration (Yang et al., 2018). Many researchers have introduced the reduction of contaminant concentration and pumping cost, or in other words the number of pumping wells and pumping rate (Zeynali et al., 2022) and some others the location of pumping wells (Sbai, 2019) and groundwater remediation time as the objective function of their optimization problem (Mategaonkar et al., 2018). Besides, researchers have used various methods such as finite difference method (He et al., 2017) finite element method (Zeynali et al., 2022) and meshfree method (Boddula and Eldho, 2017) (Seyedpour et al., 2019) and MODFOLW software (Joswig et al., 2017) (Singh et al., 2011) to solve the optimization problem of groundwater remediation. Younes et al. (2022) present a robust upwind MFE scheme is proposed to avoid such unphysical oscillations. The new scheme is a combination of the upwind edge/face centred Finite Volume (FV) method with the hybrid formulation of the MFE method (Jafarzadeh et al., 2021). The scheme ensures continuity of both advective and dispersive fluxes between adjacent elements and allows to maintain the time derivative continuous, which permits employment of high order time integration methods via the Method of Lines (Younes et al., 2022). After reviewing the literature on the subject and the research background presented, in general, it can be said that by considering different objectives simultaneously to solve the optimization problem of the PAT system, a general and appropriate design for this remediation system can be presented. Therefore, the objectives of this research include investigating the efficiency of the finite element method in solving the equations related to contaminant transport and its integration with meta-heuristic algorithms to solve the pump and treat optimization problem. Also in this research, for the optimal design of the PAT system or, in other words, determining the optimal location of injection pumping wells, objectives such as minimizing human health risk, reducing head drawdown and reducing the pumping rate of polluted water are considered as single, double and triple objectives. To investigate the single-objective optimization problem, hybrid GA-FEM, PSO-FEM and MVO-FEM models are used. To solve the multi-objective optimization problem, NSGA-II-FEM, MOPSO-FEM and MOMVO-FEM models are also used.

2. Material and Methods

2.1. Case Study

In this study, a hypothetical aquifer is considered. This hypothetical aquifer is almost similar to the confined aquifer considered by Sharief (Sharief et al., 2008). In the hypothetical aquifer, the length of the aquifer is 1800 meters and its width is 1000 meters (Fig. 1). The hydrogeological parameters taken for the aquifer are as given in Table 1). The entire aquifer has storativity of 0.0004 and a pond is located in zone A, the seepage rate of which is 0.009 m/day. Zone A and Zone C are assumed to be recharged at a rate of 0.00024 and 0.00012 m/d, respectively, as seen from Fig. 1.
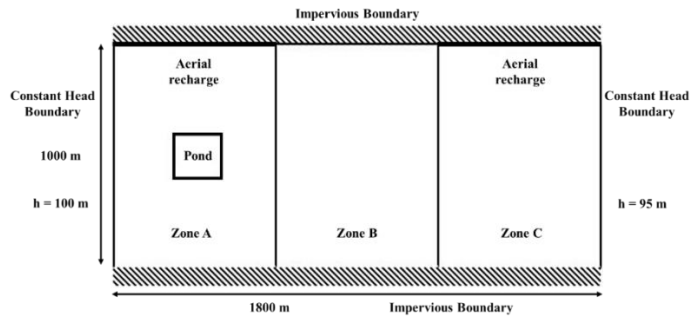
Fig. 1. Hypothetical confined aquifer configuration

Table 1. Hydrogeological data used for the coupled flow and transport model

Properties	Zone A	Zone B	Zone C
Transmissivity T_x (m²/d)	500	400	250
Transmissivity T_y (m²/d)	300	250	200
Porosity	0.20	0.25	0.15
Longitudinal dispersivity (m)	150	75	50
Transverse dispersivity (m)	12.5	7.5	5.0

Initially, the entire aquifer is assumed to be unpolluted. The flow model has constant head conditions in the western and eastern borders with 100 and 95 meters, respectively, and no flow boundaries in northern and southern directions. For the contaminant transport model, only the eastern boundary is kept open and all other boundaries are considered impervious. This problem is done using the Galerkin finite element method and the Crank-Nicholson time scheme with a regular distribution of nodes in the form of 6×10 and 90 square elements (Fig. 2). The time step of 5 days is selected for both groundwater flow and contaminant transport models, and the contaminant seepage from the contaminant source is assumed to be continuous, and the contaminant concentration distribution is simulated using the FEM model.
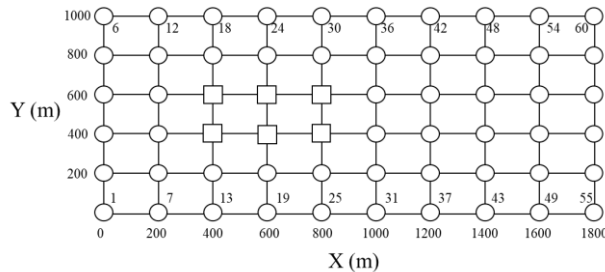

Fig. 2. FEM Mesh for Hypothetical Aquifer

2.2. Optimization problem

In this optimization problem, it is assumed that the contaminant source is a landfill. Heavy metals have been seepage from this landfill for 30 years. Contaminant seepage into the aquifer and contaminate the groundwater. Contaminant concentration and its permissible limit are given in Table 2.

Table 2. Contaminant seepage to aquifer in optimization problem

Contaminant	Value	Permissible limit	Unit
Zinc	240	200	μg/lit
Copper	240	200	μg/lit
Nickel	230	200	μg/lit
Chrome	120	100	μg/lit
Cadmium	12	10	μg/lit

In this problem, four pumping wells are used to apply the pumping and treatment policy. In the first step, the remediation period is considered to be 10 years. To monitor and compare the

results of the models, six nodes 15, 16, 21, 22, 27 and 28, which are shown as squares in Fig. 2, are considered.

2.3. Objective functions

The cost of remediation depends on the permissible limit of contaminants; high costs must always be incurred to achieve a low level of pollution. In case of non-payment, the desired level of pollution concentration cannot be reached. On the other hand, contaminants in groundwater can endanger human health. Therefore, in this research, the objective function is to determine the optimal location of pumping wells so that is minimized the carcinogenic health risk. In the single-objective problem, four wells are used with a pumping rate of 600 m³/day. The two-objectives problem, in addition to the first objective function, Minimizing the drawdown of the aquifer head is also considered with the same four pumping wells with a pumping rate of 600 m³/day. In the three-objectives minimization problem, the average pumping rate from four pumping wells is also added to the set of objective functions. Hence, the optimization functions are defined as follows:

(1)
$$Min \quad F_1 = \left(\sum_{k=1}^{K} ELCK_k \right) / K$$

(2)
$$Min \quad F_2 = \sum_{i=1}^{NNODE} \left(H_i^{old} - H_i^{new} \right)$$

(3)
$$Min \quad F_3 = \frac{\sum_{j=1}^{J} q_j^{Ex}}{J}$$

Where F_1, F_2 and F_3 are the first, second and third objective functions, respectively. In the first objective function, the carcinogenic health risk of contamination in the kth monitoring well and K is the number of monitoring wells. In the second objective function, H_i^{old} and H_i^{new} are aquifer head before and after installing pumping wells at i^{th} node and NNODE are the total number of nodes in the hypothetical aquifer domain. In the third objective function, is the mean of pumping rate from all pumping wells (m3/day). J represents the number of pumping wells and q_j^{Ex} is the pumping rate for the jth pumping well (m3/day). In addition, the

limitations of the PAT optimization model are as follows (Yang et al., 2018) (Eq. 1-8):

(4)
$$c_k^{\left(q_j^{Ex} \right)} \le c_{max} \quad k = 1, 2, ..., K$$

(5)
$$0 \le q_j^{Ex} \le q_{max}^{Ex} \quad j = 1, 2, ..., J$$

(6)
$$ELCK_k \le ELCK_{max} \quad k = 1, 2, ..., K$$

(7)
$$ELCK_k = SF \times CDI_k$$

(8)
$$CDI_k = CW_k / 1000 \times IR \times EF \times ED / (AT \times BW)$$

In which, q_{max}^{Ex} is the maximum pumping rate from the jth pumping well (m³/hr). c_k contaminant concentration in the kth monitoring well ($\mu g / lit$). Also, c_{max} is the maximum contaminant concentration ($\mu g / lit$). $ELCK_{max}$ is the maximum level of carcinogenic contamination at human health risk. SF is the slope factor that depends on the carcinogenic contamination in human health risk ($\left(mg / kg\, day \right)^{-1}$). CDI_k is contaminant drawn up around position k ($mg / kg / day$), CW_k is contaminant concentration around position k ($\mu g / lit$), IR is Ingestion rate ($mg / kg / day$), EF is frequency of exposure ($mg / kg / day$), ED is duration of exposure (year), AT average time (day) and BW is body weight (kg) (Eq. 13).

2.4. The governing equation for groundwater flow and transport

2.4.1. The governing equation for groundwater flow
The governing partial differential equations describing the steady-state flow in a two-dimensional inhomogeneous, anisotropic confined and unconfined aquifers are given as (Wang and Anderson, 1995) (Eq. 9 & 10).

(9)
$$\frac{\partial}{\partial x}\left(T_x \frac{\partial H}{\partial x} \right) + \frac{\partial}{\partial y}\left(T_y \frac{\partial H}{\partial y} \right) + \frac{\partial}{\partial z}\left(T_z \frac{\partial H}{\partial z} \right) = R$$

(10)
$$\frac{\partial}{\partial x}\left(k_x H \frac{\partial H}{\partial x} \right) + \frac{\partial}{\partial y}\left(k_y H \frac{\partial H}{\partial y} \right) + \frac{\partial}{\partial z}\left(k_z H \frac{\partial H}{\partial z} \right) = R$$

Moreover, the governing partial differential equations describing the Transient flow in a two-dimensional inhomogeneous, anisotropic confined and unconfined aquifers are given as (Wang and Anderson, 1995) (Eq. 11 & 12).

(11)

$$\frac{\partial}{\partial x}\left(T_x \frac{\partial h}{\partial x}\right) + \frac{\partial}{\partial y}\left(T_y \frac{\partial h}{\partial y}\right) = S\frac{\partial h}{\partial t} + Q_w\,\delta(x-x_i)(y-y_i) - q$$

(12)

$$\frac{\partial}{\partial x}\left(K_x h \frac{\partial h}{\partial x}\right) + \frac{\partial}{\partial y}\left(K_y h \frac{\partial h}{\partial y}\right) = S_y\frac{\partial h}{\partial t} + Q_w\,\delta(x-x_i)(y-y_i) - q$$

Where h(x,y,t) or H(x,y,t) is the piezometric head [L], $T_i(x,y)$ is anisotropic transmissivity [L^2T^{-1}]; $K_i(x,y)$ is anisotropic hydraulic conductivity [LT^{-1}]; S(x,y) is storage coefficient, $S_y(x,y)$ is specific yield; Q_w is source or sink function; ($-Q_w$ = source and Q_w = sink) [LT^{-1}]; δ is Dirac delta function; x_i and y_i are the pumping or recharge well location; q(x,y,t) is vertical inflow rate [LT^{-1}]; x and y are horizontal space variables [L] and t is the time [T].

2.4.2. FEM to solve governing equations for groundwater flow

Using Galerkin's finite element method and two-dimensional element for approximation Eq. 13, the first step is to define a trial solution.

(13)

$$\hat{h}(x,y,t) = \sum_{L=1}^{NP} h_L(t) N_L(x,y)$$

Where hL is the unknown head, NL is the known basis function at node L, and NP is the total number of nodes in the hypothetical aquifer domain. A set of simultaneous equations is obtained when residuals weighted by each of the basis function are forced to be zero and integrated over the entire domain Ω. Thus, Eq. 13 can be written as:

(14)

$$\iint_\Omega \left[\frac{\partial}{\partial x}\left(T_x\frac{\partial h}{\partial x}\right) + \frac{\partial}{\partial y}\left(T_y\frac{\partial h}{\partial y}\right) - Q_w + q - S\frac{\partial h}{\partial t}\right] N_L(x,y)\,dxdy = 0$$

(15)

$$\sum_e \iint \left(T_x^e \frac{\partial \hat{h}^e}{\partial x}\left\{\frac{\partial N_L^e}{\partial x}\right\} + T_y^e \frac{\partial \hat{h}^e}{\partial y}\left\{\frac{\partial N_L^e}{\partial y}\right\}\right) dxdy + \sum_e \iint \left(S\frac{\partial \hat{h}^e}{\partial t}\right)\{N_L^e\}dxdy$$

$$= \sum_e \iint (Q_w)\{N_L^e\}dxdy - \sum_e \iint (q)\{N_L^e\}dxdy$$

$$\{N_L^e\} = \begin{Bmatrix} N_i \\ N_j \\ N_m \\ N_n \end{Bmatrix}$$

Where .

For each component, equation (15) can be written in matrix form:

(16)

$$\left[G^e\right]\{h_I^e\} + \left[P^e\right]\left\{\frac{\partial h_I^e}{\partial t}\right\} = \{f^e\}$$

Where I = i, j, m, n are four nodes of rectangular elements and G, P, f are the element matrices known as conductance, storage matrices, and recharge vectors, respectively. Summation of

elemental matrix Eq. 16 for all the elements gives the global matrix as:

(17)

$$[G]\{h_I\} + [P]\left\{\frac{\partial h_I}{\partial t}\right\} = \{f\}$$

Applying the implicit finite difference scheme for $\dfrac{\partial h_I}{\partial t}$, term in time domain for Eq. 17 gives.

(18)

$$[G]\{h_I\}_{t+\Delta t} + [P]\left\{\frac{h_{t+\Delta t} - h_t}{\Delta t}\right\} = \{f\}$$

The subscripts t and t + Δt represent the groundwater head values at earlier and present time steps. By rearranging the terms of Eq.18, the general form of the equation can be given as:

(19)

$$\left[[P] + \omega\Delta t[G]\right]\{h\}_{t+\Delta t} = \left[[P] - (1-\omega)\Delta t[G]\right]\{h\}_t + \Delta t(1-\omega)\{f\}_t + \omega\{f\}_{t+\Delta t}$$

Where Δt = time step size, $\{h\}_t$ and $\{h\}_{t+\Delta t}$ are groundwater head vectors at the time t and t + Δt, respectively, x is Relaxation factor which depends on the type of finite difference scheme used. For fully explicit scheme $\omega = 0$; Crank–Nicolson scheme $\omega = 0.5$; fully implicit scheme $\omega = 1$.

2.4.3. The equation governing transport

The differential equation governing transport is written as follows:

(20)

$$R\frac{\partial C}{\partial t} = \frac{\partial}{\partial x}\left(D_x\frac{\partial C}{\partial x}\right) + \frac{\partial}{\partial y}\left(D_y\frac{\partial C}{\partial y}\right) + \frac{\partial}{\partial z}\left(D_z\frac{\partial C}{\partial z}\right)$$

$$-v_x\frac{\partial C}{\partial x} - v_y\frac{\partial C}{\partial y} - v_z\frac{\partial C}{\partial z} - R\lambda C$$

Equation (20) is a three-dimensional equation that governs the transport and dispersion of contaminant in groundwater sources, which also has a delay factor $R = 1 + \dfrac{\rho_b k_d}{n}$.

where C(x,y,t) is the solute concentration [ML^{-3}], D_x and D_y are the components of the diffusion coefficient with the dimensional equation [L^2T^{-1}]. l reaction rate constant [T^{-1}], w elemental feeding rate [LT^{-1}] with soluble concentration c', b thickness of the aquifer under the element [L], $R = 1 + \dfrac{\rho_b K_d}{\theta}$ delay factor with ambient mass concentration and K_d absorption coefficient [L^3M^{-1}] and q_w Specific pumping rate from a source [LT^{-1}].

2.4.4. Finite element method to solve the governing equation of transport

In the finite element method, by using an imaginary computational grid, the solution domain is connected to a number of sub-domains or elements at nodal points. Then the contaminant concentration (C_L) is calculated at nodal points. For each given point, the concentration value can be approximately calculated as follows:

(21)

$$C(x,y,z,t) = \sum_{L=1}^{NNODE} C_L(t).N_L(x,y,z)$$

Where $N_L(x,y,z)$ is an arbitrary approximation function, called the node shape function L.

Using the finite element method in equation (21) leads to a set of simultaneous algebraic equations as follows.

(22)

$$[A]\{C\}^{t+\Delta t} = [B]\{C\}^t + \{f\}$$

Where:

(23)

$$[A] = [G] + [U] + [F] + \frac{1}{\Delta t}[P]$$

(24)

$$[B] = \frac{1}{\Delta t}[P]$$

Δt the time interval is called the time step. $\{C\}^t$ The known concentration vector is at the beginning of the time step and $\{C\}^{t+\Delta t}$ the unknown concentration vector is at the end of the time step. [G], [U], [F] and [P] are square matrices whose number of rows and columns are equal to the number of nodes in the computing network. The elements of these matrices are calculated as follows.

(25)

$$G_{(L,i)}^e = \iint_e \left(D_x \frac{\partial N_i^e}{\partial x} \frac{\partial N_L^e}{\partial x} + D_y \frac{\partial N_i^e}{\partial y} \frac{\partial N_L^e}{\partial y} + D_y \frac{\partial N_i^e}{\partial y} \frac{\partial N_L^e}{\partial y} \right) dxdydz$$

(26)

$$P_{(L,i)}^e = \iint_e R.N_i^e N_L^e dxdydz$$

(27)

$$U_{(L,i)}^e = -\iint_e \left(V_x^e \frac{\partial N_i^e}{\partial x} N_L^e + V_y^e \frac{\partial N_i^e}{\partial y} N_L^e + V_z^e \frac{\partial N_i^e}{\partial z} N_L^e \right) dxdydz$$

(28)

$$F_{(L,i)}^e = -\iint_e R.\lambda.N_i^e N_L^e dxdydz$$

{f} is the input or output concentration flux vector from the boundary, which is calculated as follows.

(29)

$$\{f\} = \int_\Gamma \left(D_x \frac{\partial \hat{c}}{\partial x} n_x + D_y \frac{\partial \hat{c}}{\partial y} n_y + D_z \frac{\partial \hat{c}}{\partial z} n_z \right) N_L d\Gamma$$

Where $\hat{c}$ it represents the given concentration value at the border node, n_i is the unit vector and Γ the boundary domain.

2.5. Meta-heuristic algorithms

2.5.1. GA and NSGA-II algorithm

In the genetic algorithm and its multi-objective version, there are phases such as crossover phase and mutation phase. In the single-objective version, how to select the best members of the population is based on the value of the objective function. The members of the population are sorted based on the value of the objective function and any member of the population who has calculated the value of the objective function less (in a minimization problem) is ranked first (Akbarpour et al., 2020). But in the NSGA-II algorithm, the way to choose the ranking of the population members is based on their placement in each front. In such a way that the members of the population who are on the first front are better than the members who are on the second front. Also, the members placed in the same front are ranked by crowding distance to other members of the population.

2.5.2. PSO and MOPSO algorithm

In the particle swarm algorithm, each particle moves with a velocity vector and goes from one point in the space of feasible solutions to another point. The velocity vector in this algorithm is influenced by three factors. 1- The best position that the particle has found so far. 2- The best position that the entire group has found so far (position of the best particle) and 3- a random vector. After calculating the velocity vector, this value is added with the position of the particle to calculate the new position of the particle (Zeynali and Shahidi, 2018). But in the multi-objective version of this algorithm, instead of the particles following the best particle, the space of feasible solutions is divided into smaller ranges and a leader is defined for each range, which is better than all the particles in that range. Therefore, the second part is the velocity vector of particles affected by these particles that are designated as leaders.

2.5.3. MVO and MOMVO algorithm

The multi-verse optimizer algorithm is inspired by three main concepts of multi-verse theory. These three concepts are white holes, black holes and wormholes. In the cyclical model of the multi-verse theory, it is argued that at the point of collision between parallel universes, big bangs or white holes are created. Black holes, which are often observed, behave completely opposite to white holes. They attract everything with their immense gravitational force. Wormholes are holes that connect different parts of a universe. Wormholes in multi-verse theory act as space or time travel tunnels where objects are able to travel instantaneously to any corner of the world (or even from one world to another) (Mirjalili et al., 2016). In order to develop the multi-objective version of MVO, a repository (archive) has been added to this algorithm. This repository stores the best non-overwhelming solutions obtained so far. The search mechanism in MOMVO is very similar to MVO, where solutions are improved using white holes, black holes, and wormholes (Mirjalili et al., 2017). Finally, the FEM model and optimization algorithms were assembled in MATLAB software.

3. Results and discussion

3.1. The results of the single objective optimization problem

In solving the present optimization problem, only the concentration of zinc, chromium, and cadmium is considered, since the concentration of copper and nickel contaminant is lower than the concentration of zinc, and their permissible limits for agriculture are also the same. When the zinc concentration reaches the permissible limit at the end of the remediation period, it can be assured that the copper and nickel concentrations have also fallen below the permissible limit. Considering the above conditions, the optimization problem is transformed into determining the location of the four extraction wells in which part of the aquifer domain to achieve the optimal (near-optimal) values for the first objective function. It should be noted that the first step in the pump-and-treat process is to remove the source of contaminant or prevent seepage, and then the pumping wells will pump contaminant from the aquifer for 10 years. Each of the algorithms was run five times with a population size of 10 and 20 iterations. The results of the five runs of each algorithm, including the best, worst, and average values of the objective function, are shown in Table 3. As can be seen in this table, the genetic algorithm with an average value of 0.0005036 has shown higher performance than the other two algorithms. Also, the performance of the algorithms at their best objective function value is shown in Fig. 3.

Table 3. Statistical characteristics of objective function in five times run for all algorithms

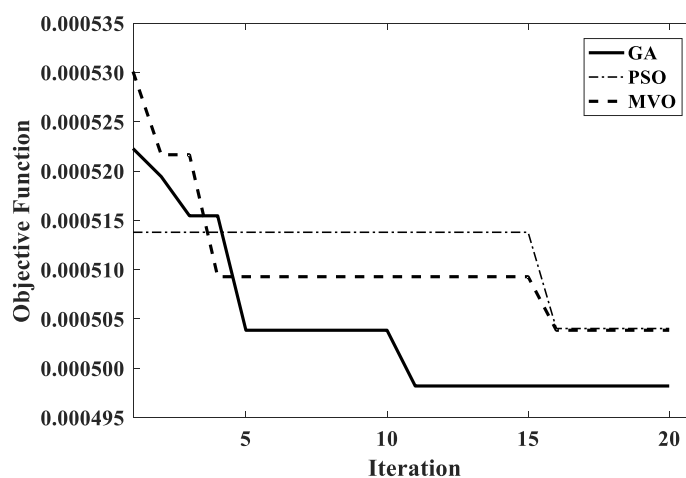| Algorithm	The best Value	The worth value	Average value
GA	0.0004982	0.0005039	0.0005036
PSO	0.0005040	0.0005239	0.0005155
MVO	0.0005038	0.0005172	0.0005091

Fig. 3. The convergance trend of Meta-Heuristic algorithms

Also, the location of the pumping wells and the concentration of Zinc contaminant in the aquifer domain after 10 years of remediation are shown in Fig. 4.
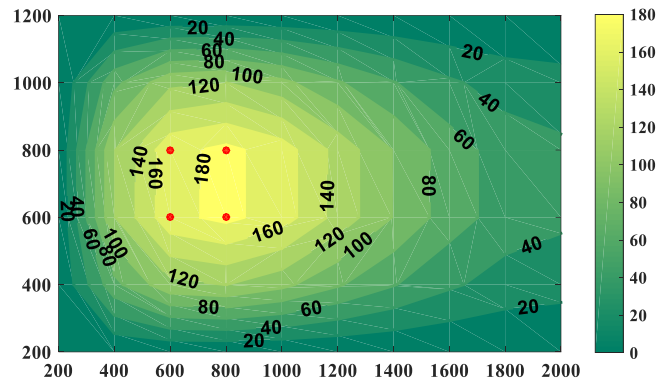

Fig. 4. Zinc contaminant concentration in aquifer domain (μg/lit) and the location of pumping wells

3.2. The results of the two-objective optimization problem

In this research, for the NSGA-II algorithm, similar to the single-objective version, 70% of the population members can act as parents, and the mutation rate is considered 90%. For the MOPSO algorithm, similar to the single-objective version, the inertia weight is 0.9, and the values of C1 and C2 are also equal to 0.51. Also, for the MOMVO algorithm, similar to the single-objective version, the parameter p is equal to six, and the values of WEPmax and WEPmin are also equal to three and zero, respectively. WEP is the probability of a wormhole. Considering the values considered, each of the algorithms was run five times, and the number of solutions that are on the Pareto front is shown in Table (4). As can be seen in this table, in the NSGA-II algorithm, the number of solutions on the Pareto front is more than the other two algorithms, and in the MOMVO algorithm, the number of solutions on the Pareto front is no more than three solutions. As an example, the distribution of solutions on the Pareto front of the NSGA-II and MOPSO algorithms in the iteration with the most solutions on the Pareto front and the last iteration of the MOMVO algorithm is shown in Fig. 5. As can be seen in Fig. 5, the MOMVO algorithm, despite the small number of solutions on the Pareto front, has provided better solutions. Therefore, it cannot be said that the number of solutions on the front is always a good criterion for determining the performance of an algorithm.

Table 4. The number of optimal pareto solutions (two objective problem)

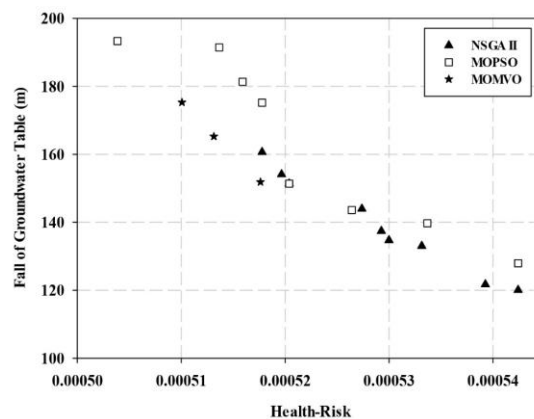| Number \ Algorithm	1	2	3	4	5
NSGA-II	7	8	4	5	9
MOPSO	4	4	3	8	6
MOMVO	3	3	3	3	3

Fig. 5. Solutions in the optimal pareto-front for all three algorithm

3.3. The results of the three-objective optimization problem

The present optimization problem with three objective functions was also investigated for a 10-year remediation period. In this problem, the location of the four pumping wells should be selected in such a way that the optimal values (as close to optimal as possible) for the carcinogenic human health risk, head drawdown, and pumping rate are achieved in the three-objective optimization problem. In the present optimization problem, each of the algorithms was run five times, and the number of solutions on its Pareto front is shown in Table 5. According to the values considered for each algorithm, the results of examining their performance showed that in all runs of the algorithms, the number of solutions on the Pareto front is more than two-thirds of the population size. Table 5 also shows that in the NSGA-II algorithm, in some cases, all members of the population are on the Pareto front. The reason for the increase in the number of solutions on the Pareto front compared to the two-objective problem can be attributed to the introduction of the third objective function. This is because in this problem, the pumping rate from each well can take on an infinite number of different values. Therefore, more solutions can be on the Pareto front. As an example, the distribution of solutions on the Pareto front for the last run of the NSGA-II algorithm is shown in Fig. 6.

Table 5. Number of optimal solution (three objective problem)

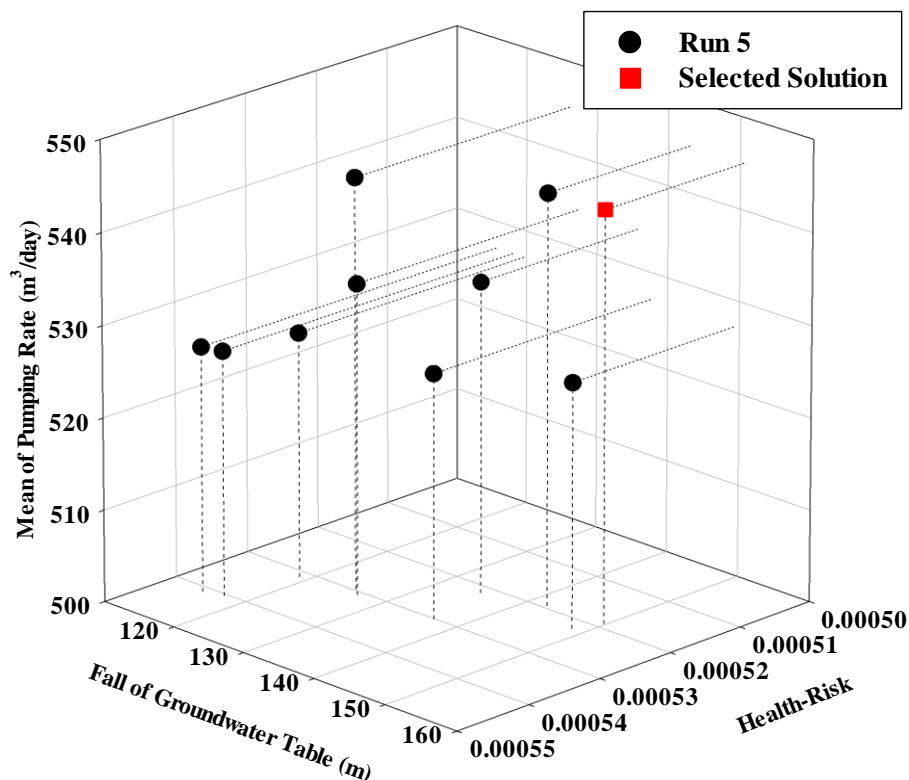| Number / Algorithm	1	2	3	4	5
NSGA-II	10	7	8	6	10
MOPSO	8	3	8	7	8
MOMVO	8	8	7	8	8

Fig. 6. Solutions in the optimal pareto-front for all NSGA-II algorithm

For the selected solution, shown as a square in Fig. 6, the pumping rate from the four pumping wells is given in Table 6 and the location of each well along with the groundwater level is shown in Fig. 7. As observed in this Fig., two pumping wells with a higher pumping rate are located in the path of the pollutant, but the other two wells, against of the results of the single-objective problem, are located at nodes closer to the left boundary (boundary with constant head) to reduce both the concentration and the groundwater head drawdown. The carcinogenic

human health risk and the concentration of each pollutant are also shown in Fig. 8 and Fig. 9, respectively. As can be seen in Fig. 8 and Fig. 9, the contaminant concentration and the carcinogenic human health rick are within the defined permissible limits.

Table 6. The value of pumping rate from four pumping well in NSGA-II algorithm

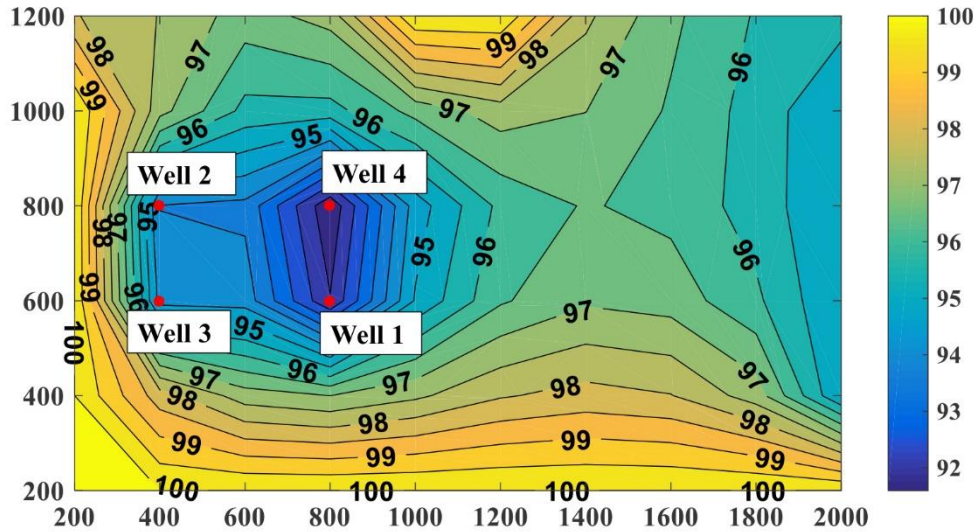| Well number	1	2	3	4
Pumping rate (m³/day)	547.60	543.24	527.44	561.95

Fig. 7. Groundwater head (meter) and four pumping well location
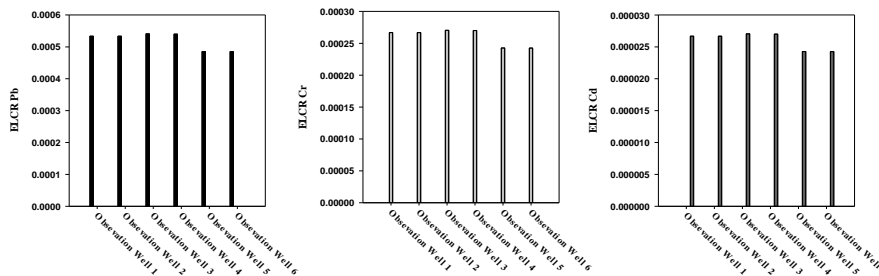

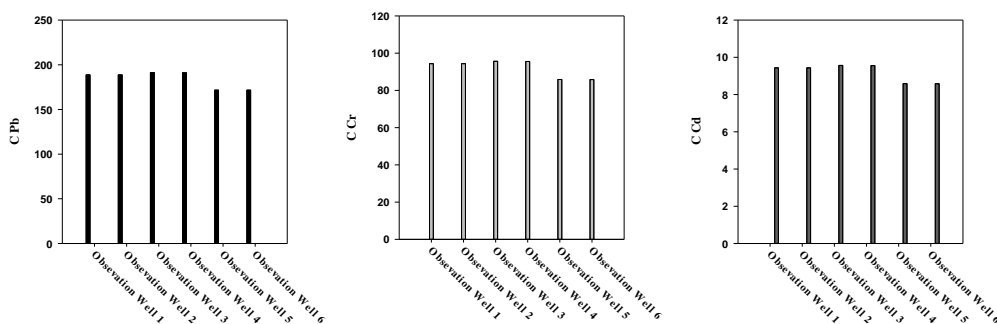**Fig. 8.** Amount of human health risk on each monitoring well

Fig. 9. Amount of heavy metals concentration on each monitoring well

4. Conclusion

In this research, hybrid optimization-simulation models GA-FEM, PSO-FEM, and MVO-FEM were used for the single-objective problem and NSGA-II-FEM, MOPSO-FEM, and MOMVO-FEM for solving multi-objective groundwater remediation optimization problems using the pump-and-treat method. The optimization problem was investigated with the mentioned models in both single-objective and multi-objective forms. In solving the single-objective optimization problem, the objective was to determine the optimal location of four pumping wells with a fixed pumping rate of 600 m³/day so that the carcinogenic human

health risk is reduced to the permissible level. The results of this section indicated that the GA-FEM model has higher efficiency than the other two models. In the two-objective problem, the groundwater level drawdown was also included as an influential parameter. The optimization problem was investigated with four pumping wells with a fixed pumping rate of 600 m^3/day. The results indicated that the number of solutions on the Pareto front is not a lot. The reason for this is the fixed pumping rate and the lack of a large number of selectable nodes. However, among the solutions provided by each model, a better solution is one that can reduce the level of pollution in the aquifer to the permissible level and, on the other hand, also minimize the groundwater level drawdown. Therefore, in general, it can be said that among the options that each algorithm provides, the option (solution) should be chosen that balances the two objective functions. This means that both the contaminant concentration and the head drawdown should be reduced simultaneously. When examining the three-objective optimization problem, due to the possibility of choosing any value for the pumping rate from each well, the number of solutions on the Pareto front was significantly more than in the two-objective problem. And sometimes it was observed that even all members of the population in the NSGA-II-FEM model were on the Pareto front. Finally, the results of this research indicated that the mentioned models are capable of solving the groundwater remediation optimization problem using the pump-and-treat method, and these models can also be used for real case studies.

Acknowledgment

References

Akbarpour, A., Zeynali, M.J. & Nazeri Tahroudi, M., 2020. Locating optimal position of pumping Wells in aquifer using meta-heuristic algorithms and finite element method. *Water Resources Management*, 34(1), 21-34.

Boddula, S. & Eldho, T.I., 2017. A moving least squares based meshless local petrov-galerkin method for the simulation of contaminant transport in porous media. *Engineering Analysis with Boundary Elements*, 78, 8-19.

Darabi, B. & Ghafouri, H., 2007. Optimal identification of ground-water pollution sources.

Eldho, T.I. & Swathi, B., 2018. Groundwater Contamination Problems and Numerical Simulation. In *Environmental Contaminants* (p. 167-194). Springer, Singapore.

Erickson, M., Mayer, A. & Horn, J., 2002. Multi-objective optimal design of groundwater remediation systems: application of the niched Pareto genetic algorithm (NPGA). *Advances in Water Resources*, 25(1), 51-65.

Freeze, R.A. & Cherry, J.A., 1979. *Ground~ ater*. Prentice-hall.

Gorelick, S.M., Voss, C.I., Gill, P.E., Murray, W., Saunders, M.A. & Wright, M.H., 1984. Aquifer reclamation design: the use of contaminant transport simulation combined with nonlinear programing. *Water Resources Research*, 20(4), 415-427.

Guneshwor, L., Eldho, T.I. & Vinod Kumar, A., 2018. Identification of groundwater contamination sources using meshfree RPCM simulation and particle swarm optimization. *Water Resources Management*, 32(4), 1517-1538.

He, L., Xu, Z., Fan, X., Li, J. & Lu, H., 2017. Meta-Modeling- Based Groundwater Remediation Optimization under Flexibility in Environmental Standard. *Water Environment Research*, 89(5), 456-465.

Jafarzadeh, A., Pourreza-Bilondi, M., Akbarpour, A., Khashei-Siuki, A. & Samadi, S., 2021. Application of multi-model ensemble averaging techniques for groundwater simulation: synthetic and real-world case studies. *Journal of Hydroinformatics*, 23(6), 1271-1289.

Joswig, P. et al., 2017. Continuously optimizing a groundwater remediation system in complex fractured media.

Kumar, D., Ch, S., Mathur, S. & Adamowski, J., 2015. Multi-objective optimization of in-situ bioremediation of groundwater using a hybrid metaheuristic technique based on differential evolution, genetic algorithms and simulated annealing. *Journal of Water and Land Development*.

Mategaonkar, M., Eldho, T.I. & Kamat, S., 2018. In-situ bioremediation of groundwater using a meshfree model and particle swarm optimization. *Journal of Hydroinformatics*, 20(4), 886-897.

Mirjalili, S., Jangir, P., Mirjalili, S.Z., Saremi, S. and Trivedi, I.N., 2017. Optimization of problems with multiple objectives using the multi-verse optimization algorithm. *Knowledge-Based Systems*, 134, 50-71.

Mirjalili, S., Mirjalili, S.M. & Hatamlou, A., 2016. Multi-verse optimizer: a nature-inspired algorithm for global optimization. *Neural Computing and Applications*, 27(2), 495-513.

Ouyang, Q., Lu, W., Hou, Z., Zhang, Y., Li, S. & Luo, J., 2017. Chance-constrained multi-objective optimization of groundwater remediation design at DNAPLs-contaminated sites using a multi-algorithm genetically adaptive method. *Journal of contaminant hydrology*, 200, 15-23.

Sbai, M.A., 2019. Well rate and placement for optimal groundwater remediation design with a surrogate model. *Water*, 11(11), 2233.

Seyedpour, S.M., Kirmizakis, P., Brennan, P., Doherty, R. & Ricken, T., 2019. Optimal remediation design and simulation of groundwater flow coupled to contaminant transport using genetic algorithm and radial point collocation method (RPCM). *Science of the Total Environment*, 669, 389-399.

Sharief, S.M.V., Eldho, T.I. & Rastogi, A.K., 2008. Optimal pumping policy for aquifer decontamination by

pump and treat method using genetic algorithm. *ISH Journal of Hydraulic Engineering*, 14(2), 1-17.

Singh, A. & Minsker, B.S., 2008. Uncertainty- based multiobjective optimization of groundwater remediation design. *Water resources research*, 44(2).

Singh, T.S. & Chakrabarty, D., 2011. Multiobjective optimization of pump-and-treat-based optimal multilayer aquifer remediation design with flexible remediation time. *Journal of Hydrologic Engineering*, 16(5), 413-420.

Wang, H.F. & Anderson, M.P., 1995. *Introduction to groundwater modeling: finite difference and finite element methods*. Academic Press.

Wang, Y., Xiao, W.H., Wang, Y.C., Wei, W.X., Liu, X.M., Yang, H. & Chen, Y., 2018. October. Simulating-optimizing coupled method for pumping well layout at a nitrate-polluted groundwater site. In *IOP Conference Series: Earth and Environmental Science* (v. 191(1), p. 012071). IOP Publishing.

Yang, A.L., Dai, Z.N., Yang, Q., Mcbean, E.A. & Lin, X.J., 2018, May. A Multi-objective Optimal Model for Groundwater Remediation under Health Risk Assessment in a Petroleum contaminated site. In *IOP Conference Series: Earth and Environmental Science* (v. 146(1), p. 012014). IOP Publishing.

Yang, A., Yang, Q., Fan, Y., Suo, M., Fu, H., Liu, J. & Lin, X., 2018. An Integrated Simulation, Inference and Optimization Approach for Groundwater Remediation with Two-Stage Health-Risk Assessment. *Water*, 10(6), 694.

Younes, A., Hoteit, H., Helmig, R. & Fahs, M., 2022. A robust Upwind Mixed Hybrid Finite Element method for transport in variably saturated porous media. *Hydrology and Earth System Sciences Discussions*, 1-29.

Zeynali, M.J., Pourreza-Bilondi, M., Akbarpour, A., Yazdi, J. & Zekri, S., 2022. Optimizing pump-and-treat method by considering important remediation objectives. *Applied Water Science*, 12(12), 268.

Zeynali, M.J., Pourreza-Bilondi, M., Akbarpour, A., Yazdi, J. & Zekri, S., 2022. Development of a contaminant concentration transport model for sulfate-contaminated areas. *Applied Water Science*, 12(7), 169.

Zeynali, M.J. & Shahidi, A., 2018. Performance assessment of grasshopper optimization algorithm for optimizing coefficients of sediment rating curve. *AUT Journal of Civil Engineering*, 2(1), 39-48.